High glucose promotes cisplatin chemoresistance in MDA-MB-231 breast cancer derived cells through changes in gene expression and multiple signaling pathways

ARACELI RUBÍ VIEDMA-RODRÍGUEZ[1], MARÍA GUADALUPE MARTÍNEZ-HERNÁNDEZ[1], LUIS ANTONIO FLORES-LÓPEZ[2], MIGUEL ÁNGEL VELÁZQUEZ-FLORES[3], RUTH RUIZ ESPARZA-GARRIDO[4], JAVIER RODRIGO PRADO-BAEZA[5] and LUIS ARTURO BAIZA-GUTMAN[1]

[1]Unit of Morphology and Function, Faculty of Higher Studies-Iztacala, National Autonomous University of Mexico, Tlalnepantla, State of Mexico 54090, Mexico; [2]Secretary of Science, Humanities, Technology and Innovation, National Institute of Pediatrics, Ministry of Health, Mexico City 04530, Mexico; [3]Non-coding RNAs Laboratory, Medical Research Unit in Human Genetics, Children's Hospital 'Dr. Silvestre Frenk Freund', National Medical Center XXI Century, Mexican Institute of Social Security, Ciudad 06720, Mexico; [4]Researchers for Mexico Program, Non-coding RNAs Laboratory, Medical Research Unit in Human Genetics, Children's Hospital 'Dr. Silvestre Frenk Freund', National Medical Center XXI Century, Mexican Institute of Social Security, Ciudad 06720, Mexico; [5]National Cancer Institute of Mexico, Mexico City 14080, Mexico

Received April 4, 2025; Accepted September 17, 2025

DOI: 10.3892/br.2025.2064

Abstract. Epidemiological and experimental evidence indicate that hyperglycemia, transient hyperinsulinemia and insulin-like growth factor-1 promote an aggressive phenotype of breast tumor cells during diabetes mellitus. The present study evaluated the effect of high glucose (HG) concentration (30 mmol/l) on cisplatin sensitivity and gene expression in MDA-MB-231 triple-negative breast cancer (TNBC)-derived cells. Cisplatin cytotoxicity was assessed by the MTT assay and was attenuated by HG. This effect was accompanied by reduced caspase-3 activation, indicating impaired apoptosis. Differentially expressed genes between HG and normal glucose (5.6 mmol/l) conditions were analyzed by microarray. The upregulation of tetraspanin 1 (*TSPAN1*) and frizzled 3 (*FZD3*) was validated by reverse transcription-quantitative PCR. HG promotes cisplatin chemoresistance by preventing apoptosis. Additionally, HG altered the expression of genes involved in glucose, glycerophospholipid, purine and pyrimidine metabolism. Regulatory pathways affected included Wnt/β-catenin, p53 network, NF-κB survival and DNA damage response. Candidate genes potentially associated with HG-induced chemoresistance included *SLC6A6, TSPAN1, TNFSF7, PDE4B, RPS13, COX4I1, RAD17, LRP8, SMARCA2, EHD1, LEF1* and *EIF4G2*. Survival analysis using the KM-Plotter platform revealed that *YBX3* and amphiregulin expression were significantly associated with poor prognosis. By contrast, amyloid precursor protein (*APP*) and N-cadherin (*CDH2*) showed non-significant trends. Coexpression analyses demonstrated that *APP* and *CDH2* were positively correlated with *YBX3*. This suggests they may contribute to tumor aggressiveness as part of *YBX3*-driven regulatory networks, rather than as independent prognostic markers. Collectively, the present findings demonstrated that HG promotes cisplatin resistance and aggressive features in TNBC cells through multiple metabolic and signaling pathways. Notably, these include the Wnt/β-catenin axis. Candidate biomarkers with potential prognostic and therapeutic relevance in diabetic breast cancer (BC) were also identified.

Correspondence to: Professor Luis Arturo Baiza-Gutman, Unit of Morphology and Function, Faculty of Higher Studies-Iztacala, National Autonomous University of Mexico, Los Reyes Iztacala, Tlalnepantla, State of Mexico 54090, Mexico
E-mail: labaiza@unam.mx

Key words: breast cancer, hyperglycemia, cell death, Wnt/β-catenin, triple-negative breast cancer

Introduction

The development of cancer is promoted by age, overweight, obesity, type 2 diabetes mellitus (T2DM) and metabolic syndrome. T2DM is associated with a significant number of cancers, such as those of the breast, pancreas, liver, colorectal, renal and reproductive systems. Diabetic patients with cancer have increased mortality compared with cancerous non-diabetic individuals (1).

Hyperglycemia, transient hyperinsulinemia, chronic inflammation and oxidative stress promote the activation of signaling mechanisms that favor the initiation, development and progression of cancer during diabetes (1,2). The increased plasma levels of insulin-like growth factors, enhanced production of inflammatory cytokines (IL-6, TNFα and IL1β), low expression of certain adipokines (adiponectin), and aberrant protein glycosylation in T2DM organisms induce changes

in metabolic and signaling pathways (2). These changes help cancer cells adapt to a hyperglycemic environment and promote the proliferation and acquisition of a migratory and chemoresistant phenotype (3). The increased proliferative activity of tumor cells depends on a continuous supply of biomolecules such as amino acids, carbohydrates, nucleotides and fatty acids capable of providing the energy requirements of the cell, favoring the synthesis of DNA, RNA, proteins and lipids at a higher rate in diabetic patients (4).

The malignant cells that survive primary treatment evolve into a population of resistant clones, leading to cancer progression and patient death (5). Mortality from breast cancer (BC) is higher in women with diabetes compared with women without it, since diabetes can exacerbate the onset and development of cancer by activating various cellular processes such as proliferation, migration and epithelial-mesenchymal transition (EMT) (6). Additionally, variations in the expression and activity of several drug-metabolizing enzymes, altered drug membrane transport, and evasion of apoptosis play a critical role in drug resistance (2).

It was found that a high concentration of glucose promotes an invasive/metastatic phenotype, inducing proliferation, migration, EMT and cell invasion in MDA-MB-231 cells, which was associated with increased expression of plasminogen activator urokinase-type (uPA), its receptor (uPAR), and type 1 inhibitor (PAI-1), leading to the activation of plasminogen activation system and AKT signaling (4,6). EMT is one of the mechanisms to enhance migratory and invasive properties of tumor cells, together with cell survival, invasiveness and chemotherapy drug resistance (7).

Elevated blood glucose levels regulate the chemoresistance in BC (2,3,8). Hyperglycemia and diabetes promote the sensitivity of BC cells or breast tumors to some DNA repair inhibitors (8). On the other hand, the development of resistance to cisplatin and other drugs by BC cells is frequently mediated by the prevention of apoptosis, increased EMT, DNA repair, Wnt and PI3K pathways, since cisplatin leads to apoptosis through increased reactive oxygen species, which leads to DNA damage (9). However, the genes and signaling pathways implicated in the development of chemoresistant and aggressive BC phenotype by high glucose (HG) in diabetic patients have not been fully explored.

It was aimed to detect the action of HG on the chemoresistance to cisplatin and changes in gene expression in MDA-MB-231 BC-derived cells. In addition, to analyze the genes, metabolic and signaling pathways that can mediate the promotion of cisplatin resistance and a migratory phenotype by HG.

Materials and methods

Cell culture. MDA-MB-231 BC cells were acquired from the American Type Culture Collection (ATCC) and cultured in Dulbecco's Modified Eagle's Medium/Ham's Nutrient Mixture F12 (DMEM-F12; MilliporeSigma). The medium was supplemented with 10% fetal bovine serum (FBS; Biowest) and the following antibiotics: penicillin 100 U/ml and streptomycin 100 μg/ml (Thermo Fisher Scientific, Inc.). The cells were authenticated by the 17 short tandem repeat profiling (ATCC Cell Line Authentication Service) in August 2020. The RNA extraction and microarray were processed in 2019, and the corresponding microarray series GSE136277 was made public in August 2019. Most of the experiments were concluded in 2020. Cultures were routinely tested for mycoplasma contamination using a PCR-based detection kit (cat. no. ab289834; Abcam). For propagation, cells were seeded and cultured in monolayers in 75-cm^2 tissue culture flasks. For some experiments, cells cultured in 6.0-cm-diameter culture plates to 60-80% confluence were cultured for 48 h in the following conditions: i) Normal glucose (NG), 5.6 mmol/l; ii) 30 mmol/l (HG); iii) HG + 60 μmol/l cisplatin (MilliporeSigma); and iv) NG + 60 μmol/l cisplatin. The cells were detached with 0.25% trypsin-EDTA solution (Biowest).

Supplementation with ~5.6 mmol/l D-glucose approximates normal blood sugar levels, whereas concentrations ~10 mmol/l and above mimic pre-diabetic and diabetic conditions, respectively. In most studies, HG conditions use 25-30 mmol/l glucose. In previous studies, it was found that 30 mmol/l glucose produced the most evident and reproducible effects on MDA-MB-231 cells (4,6). Furthermore, interstitial glucose can be similar to blood glucose, considering that interstitial glucose concentrations in skeletal muscle of patients with T2DM during a glucose tolerance test were similar to blood glucose levels (10).

MTT assay. The MTT method is a quantitative colorimetric assay that measures the metabolic activity of cells, which is proportional to changes in the cell populations. This assay was used to determine the changes in the cell population and the median lethal concentration (LC_{50}) of cisplatin under standard culture (17.5 mmol/l glucose), NG and HG conditions, and using an osmotic control of glucose 5.6 mmol/l plus mannitol 19.4 mmol/l (Mannitol). A total of 5,000 cells per well were seeded in 96-well plates and exposed to different concentrations of cisplatin (15-90 μmol/l). The culture medium was replaced with 200 μl serum-free DMEM and 50 μl of MTT solution (5 mg/ml) after 48 h of incubation at 37˚C. Then, the cells were incubated for an additional 4 h, the medium was removed, and 100 μl of dimethyl sulfoxide was added to dissolve the formazan crystals. The plate was read at 570 nm wavelength using a microplate reader iMark (Bio-Rad Laboratories, Inc.).

Western blotting. The cells were washed with PBS and lysed in RIPA Buffer (cat. no. 89900; Thermo Fisher Scientific, Inc.), containing a protease inhibitor cocktail (cat. no. I3786; MilliporeSigma) to prevent protein degradation. Proteins were quantified by the Bradford assay, and the cell lysates were stored at -70˚C. Equal amounts of protein (100 μg per well) were mixed with Laemmli sample buffer and separated by 10% SDS-polyacrylamide gel electrophoresis. The transfer was realized in a PVDF membrane (0.8 mm/cm^2, 2 h), using Tris buffer 25 mmol/l, glycine 192 mmol/l and methanol 20%. Membranes were then blocked with 5% BSA in TBS for 1 h at room temperature to prevent non-specific binding. Subsequently, membranes were incubated overnight at 4˚C with primary anti-caspase-3 antibody (1:500; cat. no. sc-7272; Santa Cruz Biotechnology, Inc.) in TBS-T (0.1% Tween-20) containing 1% BSA. Antibody binding was detected using an HRP-conjugated secondary antibody (1:5,000; cat. no. 7076S;

Cell Signaling Technology, Inc.), incubated for 1 h at room temperature, followed by visualization with an enhanced chemiluminescence kit (Clarity Western ECL substrate, Bio-Rad Laboratories, Inc.), according to the manufacturer's instructions. The images were obtained using the C-Digit Blot Scanner (LI-COR Biosciences). The bands were quantified by densitometry analysis using the Image Studio 4.0 software (LI-COR Biosciences).

RNA extraction. Total RNA was extracted using TRIzol (Invitrogen; Thermo Fisher Scientific, Inc.), according to the manufacturer's instructions. RNA quality was verified by 2% agarose gel electrophoresis, followed by ethidium bromide staining and visualization under UV light and quantified using a NanoDrop ND-1000 spectrophotometer (Thermo Fisher Scientific, Inc.).

Hybridization and microarray analysis. A total of 10 μg of total RNA obtained from cells cultured in NG and HG media was used for cDNA synthesis and labeling with the Superscript II kit (Invitrogen; Thermo Fisher Scientific, Inc.), incorporating dUTP-Cy5 for HG samples and dUTP-Cy3 for NG (control) samples. The absorbance was measured at 655 nm for Cy5 and 555 nm for Cy3. Fluorophore-labeled cDNAs were hybridized in similar quantities to the Human 10K 50-mer oligonucleotide collection (MWG Biotech Oligo Bio Sets).

Microarray images were acquired and quantified using a ScanArray 4000 scanner with QuantArray software (Packard BioChips; PerkinElmer, Inc.), and data were analyzed using Array-Pro Analyzer software (Media Cybernetics, Inc.). Background correction, normalization, intensity filtering, replicate analysis, and the selection of differentially expressed genes were performed using genArise, a free program developed by the Computing Unit of the Cellular Physiology Institute, National Autonomous University of Mexico (http://www.ifc.unam.mx/genarise/). The data generated in the present study were deposited in Gene Expression Omnibus (GEO) platform under accession number GSE136277 (https://www.ncbi.nlm.nih.gov/geo/query/acc.cgi?acc=GSE136277). Differentially expressed genes were identified using the following statistical cutoffs: Z-score ≥2 or ≤-2 for biological significance, and a false discovery rate (FDR) ≤0.05 to account for multiple testing. These thresholds were applied from the outset of the analysis to ensure the robustness of the candidate genes included in subsequent evaluations.

Reverese transcription-quantitative PCR (RT-qPCR). The microarray analysis was validated by RT-qPCR for frizzled 3 (*FZD3*) and tetraspanin 1 (*TSPAN1*). Total RNA (1 μg) was reverse-transcribed using the SuperScript™ III First-Strand Synthesis System (Invitrogen; Thermo Fisher Scientific, Inc.) according to the manufacturer's protocol (50˚C for 60 min, followed by enzyme inactivation at 70˚C for 15 min). Alternatively, when individual components were used, reverse transcription was performed in a 20 μl reaction mixture containing 200 U M-MLV reverse transcriptase, 1X first-strand buffer, 0.5 mM dNTP mix (Thermo Fisher Scientific, Inc.), 25 μg/ml oligo(dT) primers (Invitrogen; Thermo Fisher Scientific, Inc.), and 40 U RNase inhibitor, incubated at 37˚C for 60 min with enzyme inactivation at 95˚C for 15 min. The resulting cDNA was amplified using the Maxima SYBR Green/ROX qPCR Master Mix (Fermentas; Thermo Fisher Scientific, Inc.) on a StepOnePlus™ Real-Time PCR System (Applied Biosystems; Thermo Fisher Scientific, Inc.).

The resulting cDNA was amplified using the Maxima SYBR Green/ROX qPCR Master Mix (Fermentas; Thermo Fisher Scientific, Inc.) in a StepOnePlus™ Real-Time PCR System (Applied Biosystems; Thermo Fisher Scientific, Inc.) with the following thermocycling conditions: Initial activation at 95˚C for 15 min; 40 cycles of 95˚C for 15 sec and annealing at the primer-specific melting temperature for 1 min; followed by a final extension at 72˚C for 10 min. Expression of the selected genes was normalized to hypoxanthine-guanine phosphoribosyltransferase (*HPRT*). The primer sequences used were as follows: *FZD3* forward, 5'-CATGGAGATGTTT GGTGTTCCTT-3' and reverse, 5'-AAGTCGAGGATATGG CTCATCAC-3'; *TSPAN1* forward, 5'-TGGGCTGCTATG GTGCTA-3' and reverse, 5'-TGCAGGTTTCATTGGCTG T-3'; and *HPRT* forward, 5'-CATTATGCTGAGGATTTG GAAAGG-3' and reverse, 5'-CTTGAGCACACAGAGGGC TACA-3'. Relative expression levels were calculated using the $2^{-\Delta\Delta Cq}$ method (11).

HPRT was used as a housekeeping gene because its expression has been considered moderately stable in BC cell lines, including MDA-MB-231 cells (12). Under hyperglycemic conditions, Liu *et al* (13) identified the *HPRT* gene as one of the more reliable reference genes in retinal pigment epithelial cells, and even *HPRT* expression was more stable than *ACTB* and *GAPDH* genes. Additionally, no changes in the expression of this gene under HG were found in our microarray study.

Immunohistochemical (IHC) expression of TSPAN-1 and FZD3 in BC tissue. IHC expression of TSPAN1 and FZD3 in *BC* tissue. To investigate the protein expression patterns of TSPAN1 and FZD3, representative IHC images of ductal breast carcinoma were analyzed from 50 samples available in the Human Protein Atlas database (https://www.proteinatlas.org/), corresponding to women aged 30-37 years. Adjacent normal breast tissue and adenoma samples were used as controls.

Gene analysis and Gene Ontology (GO). The analysis of genes differentially regulated by HG and their associated functions, including GO categories (cellular components, molecular functions and biological processes), as well as biological pathways, was performed using Gene Set Enrichment Analysis (GSEA). For this purpose, the WEB-based GEne SeT AnaLysis Toolkit (WebGestalt; http://www.webgestalt.org/) and WikiPathways Cancer were employed. Gene sets were considered significant at an FDR ≤0.05. In addition, Kyoto Encyclopedia of Genes and Genomes (KEGG) pathway analysis (https://www.genome.jp/kegg/pathway.html) was used to determine the interactions of differentially expressed genes within metabolic and signaling pathways.

Functional association network and selection of genes involved in chemoresistance. All the overexpressed and downregulated genes associated with cancer were uploaded into the program STRING (https://string-db.org/), which predicts the protein-protein interaction (PPI) network. The confidence

score for displaying interaction was 0.9. The formatted PPI networks were uploaded and visualized with the Cytoscape software (version 3.10.1) (14). Due to the complexity of this network, the CytoHubba plugin was used to select the 50 nodes with the highest degree score, and their interaction network was constructed (15). Furthermore, the overexpressed genes with at least 2-fold change and their involvement in chemoresistance, according to scientific studies (16-19), were selected, and their possible participation in HG-dependent chemoresistance was considered.

Kaplan-Meier (KM) plot analysis. Overall survival (OS) analysis was performed for the key genes *YBX3* (also known as *CSDA*), amphiregulin (*AREG*), amyloid precursor protein (*APP*) and N-cadherin (*CDH2*) using the KM Plotter database (20); (https://kmplot.com) to assess the prognostic value of the genes associated with cisplatin resistance in BC. A cohort of 153 patients with TNBC who were split into high and low expression groups was selected, considering the median expression of the gene. OS plots were created using data from BC samples negative for estrogen, progesterone and HER2 receptors, as detected by IHC and microarray. The hazard ratio (HR) with 95% confidence intervals (CIs) and log-rank P-values were calculated.

Coexpression analysis. To evaluate whether the selected genes are coexpressed in a cohort of patients with BC and the potential molecular and regulatory interactions between proteins codified by them, the coexpression of *AREG*, *FZD3*, *APP* and *CDH2* with *YBX3* was performed using R2: Genomics Analysis and Visualization Platform (http://r2.amc.nl) on TCGA Breast Invasive Carcinoma (BRCA) datasets (1,097 samples) with R2 internal identifier ps_avgpres_tcgabrca1097_tcgars. Pearson correlation coefficients and associated P-values were calculated, with scatter plots and linear regression used for visualization.

Statistical analysis. All experiments were performed in at least three independent replicates. Data are expressed as the mean ± SD. One-way ANOVA followed by Tukey's multiple comparison test was used for MTT, western blotting and RT-qPCR analyses, and performed using GraphPad Prism 8.02 software (Dotmatics). $P \leq 0.05$ was considered to indicate a statistically significant difference. Microarray and GSEA analyses were considered significant with fold-change ≥1.5 and FDR≤0.05, respectively. Co-expression analyses of *AREG*, *FZD3*, *APP* and *CDH2* with *YBX3* were performed using the R2 Genomics platform https://hgserver1.amc.nl/cgi-bin/r2/main.cgi, and survival analyses were conducted using the KM Plotter, with HRs, 95% CIs and log-rank P-values. $P \leq 0.05$ was considered to indicate a statistically significant difference.

Results

Previously, it was found that HG increases cell population growth, migration, invasion and EMT in MDA-MB-231 cells (4). In the present study, the effect of HG was analyzed on cisplatin resistance, cell death and changes in gene expression. Additionally, it was analyzed how the change in gene expression is associated with a chemoresistant and aggressive phenotype.

Hyperglycemia-induced resistance to cisplatin. To investigate whether HG induces drug resistance, the LC_{50} of cisplatin for MDA-MB-231 cells was determined under standard culture conditions (glucose 17.5 mmol/l), NG, NG with mannitol (osmotic control) and HG. The osmotic control group showed no difference compared with the NG group. Cell viability progressively decreased as cisplatin concentration increased from 15 to 90 μmol/l in a concentration-dependent manner, with LC_{50} values of 60, 15 and 75 μmol/l for standard, NG and HG conditions, respectively. These findings indicated that cells cultured under HG and standard conditions were more resistant to cisplatin compared with those cultured under NG. Thus, in the present study, cisplatin resistance was directly proportional to glucose concentration (Fig. 1A and B).

Hyperglycemia prevents the apoptosis induced by cisplatin. Apoptosis induced by cisplatin under normoglycemic and hyperglycemic conditions was evaluated in MDA-MB-231 cells by western blot analysis of caspase-3 activation. The caspase 3 antibody recognizes two band, one of higher molecular weight (MW) corresponding with the procapase 3, and other of lower MW corresponding to the cleaved/active caspase 3 (Fig. 1C). Both NG and HG groups exhibited similar levels of total caspase 3 independently of the cisplatin treatment (Fig. 1D). Whereas, cisplatin induced a significant increase in the proportion of active caspase 3 in both NG ($P \leq 0.001$) and HG ($P \leq 0.001$) conditions (Fig. 1E). Notably, the NG and NG/cisplatin groups displayed higher levels of active caspase-3 than the corresponding HG and HG/cisplatin groups (Fig. 1E). These results indicated that HG attenuated cisplatin-induced apoptosis, thereby promoting cisplatin chemoresistance.

Overall changes in gene expression. Considering an expression change equal to or greater than 1.5-fold, 1,099 genes were differentially expressed. Among these, 457 were overexpressed, while 642 were downregulated under the HG condition. The top 15 overexpressed and downregulated genes in the HG microenvironment are presented in Table I. All differentially expressed genes are listed in Tables SI and SII.

GSEA. Microarray data were subjected to functional enrichment analysis using WEB-Gestalt and the WikiPathways database. In the cellular component analysis, an activation of genes that encode protein constituents of the ribosomes, plasma membrane, cell junctions and endoplasmic reticulum was found (Fig. 2A). This was also reflected in the molecular function analysis, where changes in structural constituents of ribosomes, sodium symporter activity and ion transmembrane transport were identified. In addition, changes in hydrolase activity, calcium ion binding, kinase binding and protein-containing complex binding were observed (Fig. 2B). According to the enrichment analysis, the following signaling pathways were enriched in a hyperglycemic microenvironment: Wnt/β-catenin, angiogenesis, TP53 network, NF-κB survival signaling, apoptosis, TGF-beta receptor signaling and ATM-dependent DNA damage response (Fig. 2C).

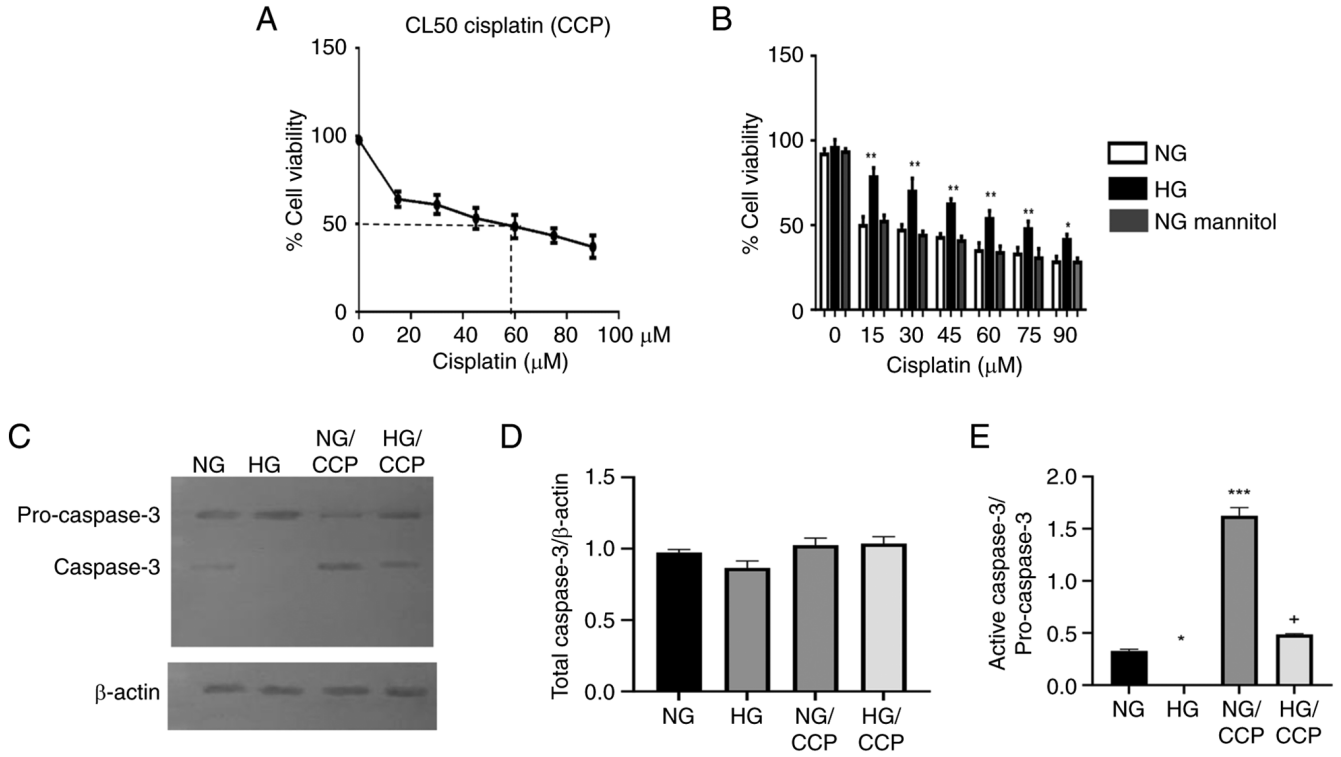


Figure 1. HG attenuates the effect of cisplatin on the cell population and prevents apoptosis. (A and B) MDA-MB-231 cells were treated for 48 h with CCP. The growth of the cell population was evaluated by the MTT assay in standard, (NG), HG, and mannitol osmotic control (NG Mannitol) culture conditions. *P≤0.01 and **P≤0.001 vs. the respective NG for each cisplatin concentration. No significant differences were observed between the NG and mannitol-treated groups. (C-E) Additionally, the activation of caspase 3 was evaluated by western blotting and densitometry in lysates of cells cultured for 48 h, in NG and HG conditions, and treated with cisplatin (NG/CCP and HG/CCP). The intensities of the bands were calculated after background subtraction, and the sum of the bands (total caspase 3) and active caspase 3 were normalized to (D) β-actin and (E) procaspase 3, respectively. Data are presented as the mean ± SD of three independent experiments. *P≤0.05 and ***P≤0.001 vs. NG, and + P≤0.001 vs. HG. HG, high glucose; NG, normal glucose; CCP, cisplatin.

Gene validation. The expression of *TSPAN1* and *FZD3* was evaluated by RT-qPCR to validate the microarray analysis. Both genes are associated with an aggressive BC phenotype and showed some of the highest Z-scores (3.81 for *TSPAN1* and 2.85 for *FZD3*). In particular, FZD3, a protein of the Wnt/β-catenin pathway, exhibited the highest Z-score. RT-qPCR analysis confirmed that *FZD3* expression under HG conditions was 3.81-fold higher compared with NG (Fig. 3). Similarly, *TSPAN1* expression under HG conditions was 2.26-fold higher than under NG conditions, consistent with the microarray results (Fig. 3). These findings are also supported by data from the Human Protein Atlas, which shows higher expression of TSPAN1 and FZD3 proteins in BC tissues compared with healthy mammary tissue (Fig. 3).

Hyperglycemia alters genes associated with metabolism. According to the aforementioned analysis with the KEGG pathways program, it was found that a high number of genes of transmembrane transporters and ribosomal proteins were differentially expressed in HG conditions (Table II). Additionally, several genes associated with other metabolic processes were found, including: i) Synthesis of DNA, RNA and proteins; and ii) purine, pyrimidine and lipid metabolism. Noteworthy, the upregulation of some genes of electron chain transport or ECT (*COX41*, *COX61*, *COX7B* and *NDUFB3*) indicated an increase in the electron flux through this chain. However, subunits *ATP5O* and *ATP5D* of the ATP synthase were downregulated, suggesting the uncoupling between the ECT and ATP synthesis.

Hyperglycemia alters genes associated with apoptosis and cell survival. On the other hand, it was found that HG induces increased expression of some genes that promote cell survival (*TNFSF7* and *TRAF1*) (21) or prevent apoptosis *(XIAP* and *BCL2L2*) (22,23). Additionally, HG leads to low expression of proapoptotic factors (*BIK, PDCD8, PDCD5, BNIP1, DAPK1* and *CCAR2*) (24-26). These data indicated that HG prevents BC cell death and promotes cell survival under stress conditions, such as the presence of chemotherapeutic agents, such as cisplatin (Fig. 1).

Signal pathways associated with the adaptation to hyperglycemia. The KEGG pathways program indicates that Wnt-β-catenin, Jak/STAT and Ras-MAPK are involved in the action of HG, together with processes such as cytokine-cytokine receptor interaction, regulation of actin cytoskeleton and focal adhesion (Table II). These results and the PPI analysis suggested that the Wnt-β-catenin signaling has a significant role in the action of HG.

Selection of hub genes and PPI. In the PPI network of over-expressed genes constructed by Cytoscape, a total of 303 nodes and 834 edges were arranged (data not shown); further analysis by cytoHubba based on this network revealed a

Table I. Top 15 upregulated and downregulated genes in a hyperglycemic environment.

ID	Genes	Z score	Full name
Upregulated			
NM_032741	*AGPAT1*	4.152511	1-Acylglycerol-3-phosphate O-acyltransferase 1
NM_003043	*SLC6A6*	4.058222	Taurine transporter
NM_005727	*TSPAN-1*	3.811546	Tetraspanin 1
NM_004189	*SOX14*	3.648091	SRY-box 14
NM_021625	*TRPV4*	3.609894	Transient receptor potential cation channel subfamily V member 4
NM_016176	*SDF4*	3.445534	Stromal cell derived factor 4
NM_006213	*PHKG1*	3.320789	Phosphorylase kinase catalytic subunit gamma 1
NM_020649	*CBX8*	3.251316	Chromobox 8
NM_001252	*TNFSF7*	3.129304	CD70 molecule
NM_005919	*MEF2B*	3.041269	BORCS8-MEF2B readthrough
NM_002600	*PDE4B*	3.035975	Phosphodiesterase 4B
NM_002150	*HPD*	2.983852	4-Hydroxyphenylpyruvate dioxygenase
NM_014610	*GANAB*	2.950495	Glucosidase II alpha subunit
NM_017412	*FZD3*	2.854118	Frizzled class receptor 3
Downregulated			
NM_006544	*SEC10L1*	-4.523611	Exocyst complex component 5
NM_012261	*LAMP5*	-4.45501	Lysosomal associated membrane protein family member 5
NM_012070	*ATRN*	-4.333672	Attractin
NM_004185	*WNT2B*	-3.908675	Wnt family member 2B
NM_001697	*ATP5O*	-3.87772	ATP synthase, H+ transporting, mitochondrial F1 complex, O subunit
NM_053004	*FLJ21125*	-3.814458	G protein subunit beta 1 like
NM_003692	*TMEFF1*	-3.744839	Transmembrane protein with EGF like and two follistatin like domains 1
NM_006866	*LILRB1*	-3.717488	Leukocyte immunoglobulin like receptor A2
NM_003072	*SMARCA4*	-3.709549	SWI/SNF related, matrix associated, actin-dependent regulator of chromatin, subfamily A, member 4
NM_021176	*G6PC2*	-3.584369	Glucose-6-phosphatase catalytic subunit 2
NM_004937	*CTNS*	-3.50955	Cystinosin, lysosomal cystine transporter
NM_004208	*PDCD8*	-3.506222	Apoptosis-inducing factor, mitochondrion-associated, 1
NM_013335	*GMPPA*	-3.505725	GDP-mannose pyrophosphorylase A
NM_017882	*CLN6*	-3.495366	Ceroid-lipofuscinosis, neuronal 6, late infantile, variant
NM_022444	*SLC13A1*	-3.435806	Solute carrier family 13 (sodium/sulfate symporters), member 1

network with 50 principal nodes (Fig. 4). Between the highest degree score hubs, genes for ribosomal proteins were found, such as *RPL13a*, *RPL23a*, *RPS3a1*, *RPS13*, *RPS8*, *RPS21*, *RPL6*, *RPL15*, *RPS7*, *MRPS7* and *RPL9* with a high degree of interaction shown in red (Fig. 3). Interacting with these nodes genes coding for transcription and protein synthesis (*PABPC1*, *EIF4G2*, *EIF5B*, *EEF1G* and *HNRNPA1*), potassium channels (*KCNG2*, *KCNG1* and *KCNS1*) and metabolism (*COX4I1*, *COX6A1* and *NDUFB3*) were found. Other important hubs were associated with the Wnt/canonical pathway, such as *WNT-1*, *DVL2* and *LEF1*. Other proteins related to cancer progression were also represented (*APP*, *AREG* and *CDH2*). It is noteworthy that ribosomal proteins were over-represented and had the highest degree scores (red and orange in Fig. 4). Because of this, nodes of important proteins had lower degree scores (orange and yellow in Fig. 4). The PPI network according to the enrichment analysis indicates the relevance of Wnt/β-catenin (Fig. 2C).

Prognostic value of Hub genes YBX3, AREG, APP and CDH2. Considering the hub genes with the highest number of interactions obtained from the CytoHubba analysis and their prognostic evaluation using the KM-plot platform, *YBX3* or *CSDA* (HR=2.04; 95% CI, 1.01-4.01; P=0.041), *AREG* (HR=2.57; 95% CI, 1.26-5.24; P=0.0073), *APP* (HR=1.73; 95% CI, 0.87-3.44; P=0.11) and *CDH2* (HR=1.74; 95% CI, 0.88-3.46; P=0.11) were associated with poor prognosis in diabetic patients with BC (Fig. 5). These data demonstrate that high expression of *YBX3* and *AREG* is significantly associated with reduced survival probability, whereas *APP* and

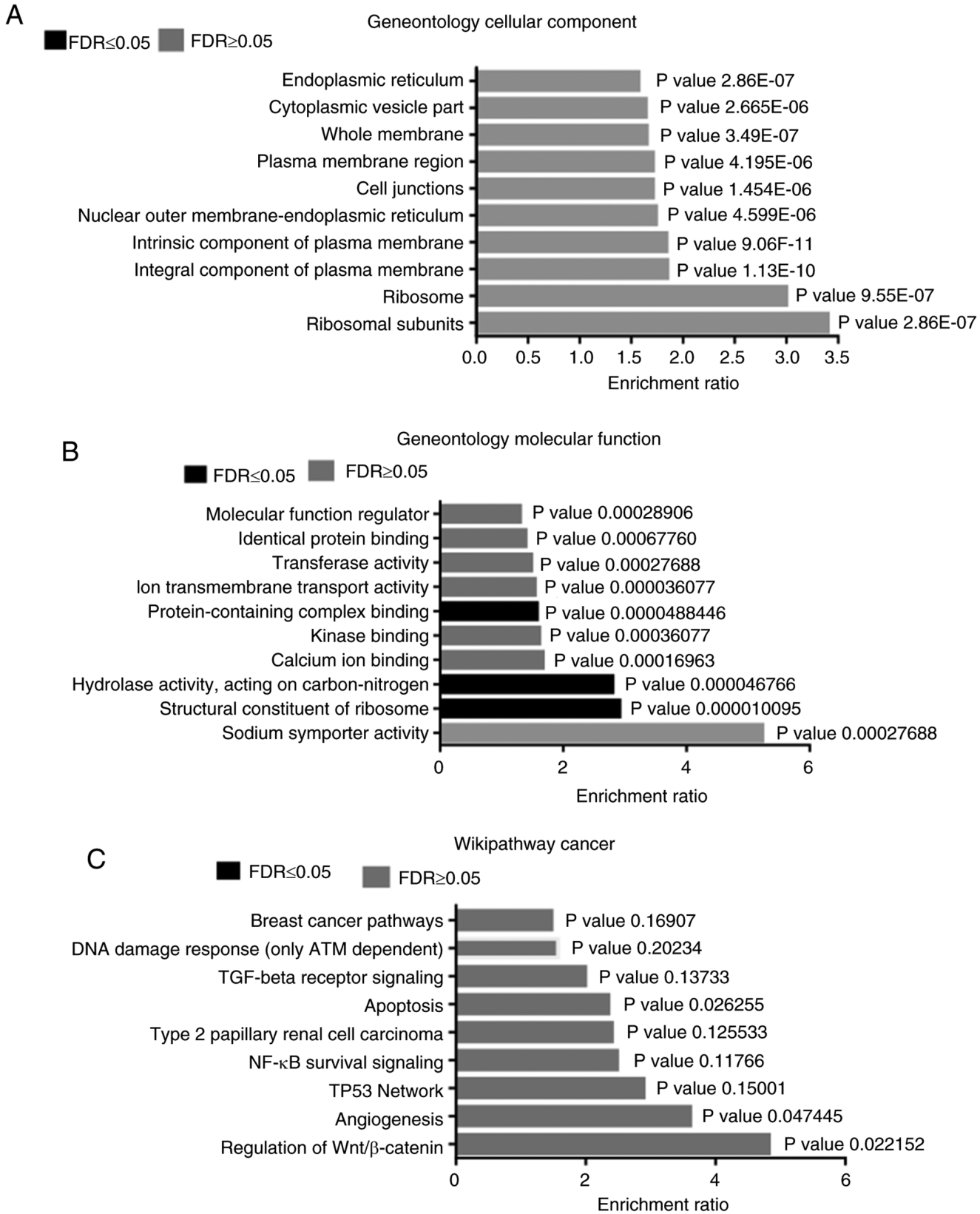


Figure 2. Gene enrichment analysis. (A and B) Gene Ontology terms of the significantly upregulated and downregulated genes for (A) the cellular components and (B) molecular function categories. (C) Wikipathways gene enrichment analysis in a hyperglycemia microenvironment.

CDH2 did not reach statistical significance. Nevertheless, elevated *YBX3* and *AREG* levels may serve as potential biomarkers for identifying diabetic patients with BC with a worse prognosis.

Coexpression of hub genes YBX3, AREG, APP and CDH2. The coexpression analysis was performed in a cohort of 1,097 patients diagnosed with breast invasive carcinoma, aged 26 to 90 years, with heterogeneous clinical

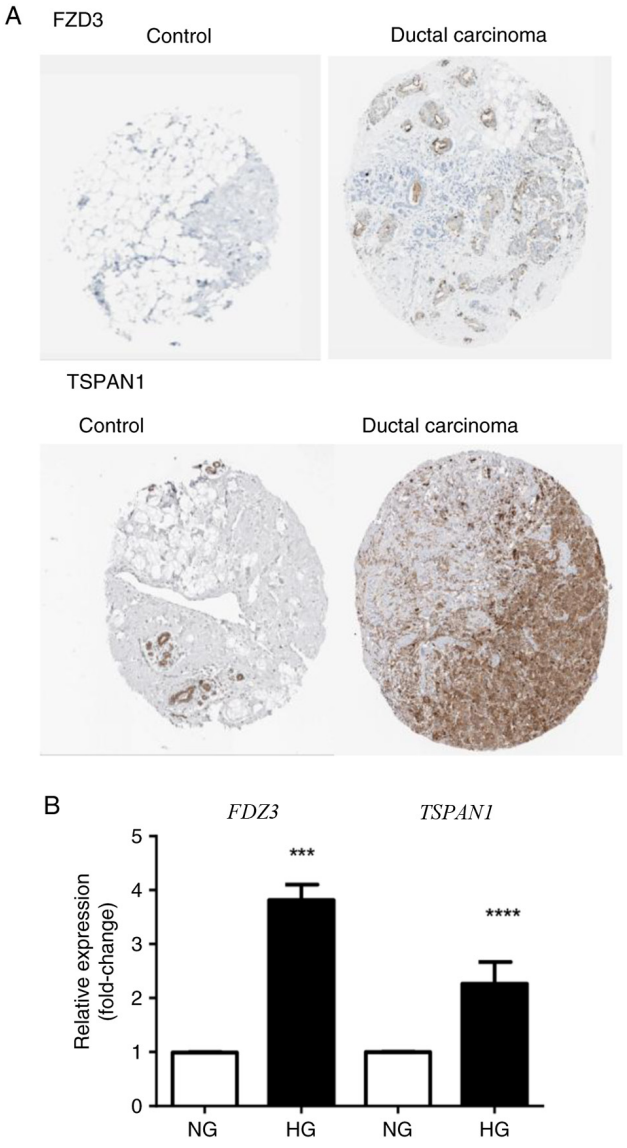


Figure 3. Expression of FZD3 and TSPAN1 in breast cancer by IHC and RT-qPCR. (A) Expression of FZD3 and TSPAN1 was analyzed by IHC using images obtained from the Human Protein Atlas. Brown staining indicates the presence of FZD3 and TSPAN1, showing higher expression in ductal carcinoma compared with control groups, including adenoma and normal breast tissue. (B) MDA-MB-231 cells were cultured in NG and HG. Total RNA was isolated 48 h after treatment, and mRNA was evaluated by RT-qPCR. These results are consistent with the microarray data. Media ± standard deviation of three experiments with two replicates each. ***P≤0.001 vs. NG. IHC, immunochemistry; RT-qPCR, reverse transcription-quantitative PCR; HG, high glucose; NG, normal glucose.

characteristics (Fig. 6), including estrogen receptor status (ER^+ 71.7%, ER^- 22%), progesterone receptor status (PR^+ 63.7%, PR^- 31.4%), HER2 status ($HER2^+$ 14%, $HER2^-$ 51.3%) and metastatic condition (M0 82.6%, MX 14.8% and M1 2%). The analysis revealed that *APP* and *AREG* expression were significantly correlated with *YBX3* (R=0.373 and R=0.119, respectively), indicating that higher *YBX3* expression is associated with increased *APP* and *AREG* expression. A positive but weak correlation was observed between *YBX3* and *FZD3* (R=0.139). Importantly, *CDH2* and *YBX3* also exhibited a weak but statistically significant correlation (R=0.131; $P=1.29x10^{-5}$).

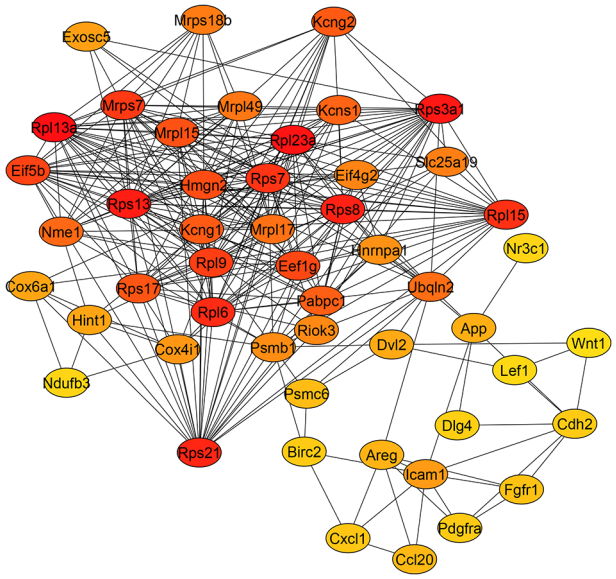


Figure 4. Major 50 hub genes interaction. These genes were selected using the String network of protein-protein interaction, considering those overexpressed with a fold change >1.5, followed by hub selection using Cytohubba. The nodes with major degree scores are shown in a decreasing scale from red to yellow. Data show gene hubs such as *BIRC2, DVL-2, WNT1* and *ATM*, which have regulatory functions associated with the WNT/β-catenin signaling pathways, apoptosis, and ATM-dependent DNA damage repair.

Discussion

Hyperglycemia is one of the most important factors considered a promoter of cancer in T2DM. In the present study, it was detected that HG induces cisplatin resistance and changes in gene expression in MDA-MB-231 cells. These changes indicate a variety of alterations in metabolic and signaling pathways that may be related to preventing cell death and increased chemoresistance associated with an aggressive phenotype. Additionally, some genes (*AREG* and *YBX3*) were selected as possible biomarkers of chemoresistance and prognostic indicators. Furthermore, it was confirmed that hyperglycemia increases the migratory phenotype in these cells.

HG induces resistance to cisplatin. The prometastatic action of HG on MDA-MB-231 cells has been demonstrated. In our previous studies, HG promoted the growth of the cell population, EMT, clonogenicity, cell migration and cell invasion compared with NG and the control of osmolality (4,6). It was also described that T2DM promoted the progression of BC in mice (27). In the present study, the lower IC_{50} for cisplatin in cell cultures with HG indicated the induction of cisplatin resistance by HG, corroborating that HG is a promoter of chemoresistance (2,3,8). Chemoresistance is associated with an invasive phenotype, and both are dependent on the prevention of apoptosis and the induction of EMT, cancer stemness, oncogenes, tumor suppressors, and metabolic and cell signaling reprogramming, involving transporter pumps, mitochondrial alterations, DNA repair and autophagy (28).

Prevention of cisplatin-induced apoptosis by HG. To confirm if the prevention of the cytotoxic effect of cisplatin by HG is due to the prevention of cell death, caspase-3 was assessed.

Table II. Kyoto Encyclopedia of Genes and Genomes pathways associated with genes regulated by hyperglycemia.

Metabolic or signaling pathway	Total genes	Genes upregulated	Genes downregulated
Transmembrane transport	27	*SLC6A6*, *SLC44A4*, *SLC35F2*, *SLC16A8*, *SLC13A2*, *SLC6A20*, *SLC23A2*, *SLC25A19*, *SLC39A7*, *SLC22A18AS*, *SLC25A5*	*SLC13A1*, *SLC22A7*, *SLC26A3*, *SLC7A7*, *SLC2A8*, *SLC35B3*, *SLC6A12*, *SLC1A7*, *SLC39A6*, *SLC39A4*, *SLC35C2*, *SLC38A3*, *SLC16A10*, *SLC44A2*, *SLC25A17*, *SLC28A2*
Cytokine-cytokine receptor interaction	24	*CXCL1*, *CXCR3*, *PDGFRA*, *IL9R*, *IL21R*, *IL1RA*, *EPOR*, *IL17RA*, *IL17RB*, *TNFSF7*, *CCL20*, *IL32*	*TNIP2*, *CCR9*, *CXCR2*, *CXCR4*, *CXCR6*, *CCRL1*, *TGFBR2*, *TGFBR1*, *CXCL6*, *IFNA8*, *IL4*, *IL17C*
Regulation of cytoskeleton	24	*CHRM4*, *FGFR1*, *PDGFRA*, *VAV3*, *CFL*, *ITGB4*, *RASAL-1*, *RIN1*, *CDC42BPA*, *RAB9A*, *RHOB*	*PIK3C2B*, *PIK3R5*, *CHRM1*, *FGF20*, *FGFR2*, *ACTN3*, *VCL*, *VAV2*, *ILK*, *ARHGDIB*, *RDX*, *RRAS*, *RASSF7*
Ribosomal proteins (extra and intramitochondrial)	20	*RPS13*, *RPS17*, *RPS21*, *RPS3A*, *RPS8*, *RPS7*, *RPL23A*, *RPL13A*, *RPL15*, *RPL9*, *MRPS18B*, *MRPS7*, *MRPL15*, *MRLP17*, *MRPL49*	*MRPS31*, *MRPL11*, *RPL23*, *MRPL33*, *MRPL42*
Purine, pyrimidine metabolism/nucleic acid synthesis	22	*XDH*, *POLA2*, *POLG*, *GUCY2F*, *PDE1B*, *PAPSS2*, *PDE2A*, *UPB1*, *PDE4B*, *ADCY7*, *NME1*, *ECGF*, *NOC3L*, *ATIC*	*CDA*, *NT5E*, *AK3*, *AMPD2*, *AMPD3*, *ADA2*, *MTAP*, *DNPH1*
MAPK	20	*FGFR1*, *PDGFRA*, *MKNK*, *DUSP4*, *RIN1*, *MAPK8IP1*, *RASGRF1*	*PPP3C*, *FGF20*, *TGFBR2*, *MAP2K3*, *MAPKAPK5*, *MEF2C*, *BLK*, *DUSP5*, *TGFBR1*, *FGFR2*, *RRAS*, *RAPGEF2*, *RASSF7*
Ras	19	*FGFR1*, *PDGFRA*, *TEK*, *RIN1*, *RASGRF1*, *SPEC1*, *RASAL-1*, *RIN1*	*PIK3C2B*, *PIK3R5*, *FGF20*, *GNB1*, *FGFR2*, *ANGPT1*, *RRAS*, *RALA*, *RAPGEF2*, *RASSF7*, *PLAAT1*
Apoptosis	19	*TRAF1*, *CASP10*, *XIAP*, *BCL2L2*, *BIRC2*, *RHOB*, *PERP*	*PTPN13*, *PIK3C2B*, *PIK3R5*, *PDCD8*, *PDCD5*, *BIRC3*, *BIK*, *DAPK1*, *CCAR2*, *BNIP1*, *TNIP2*, *RASSF7*
Wnt β-catenin	17	*FZD3*, *FZD4*, *LPR8*, *DVL2*, *WNT1*, *LEF1*, *DKKL1*, *RHOB*, *PPP2R3B*	*WNT2B*, *TGFBR2*, *BMP2*, *TGFBR1*, *ID1*, *PPP3CA*, *TBL1*, *CAMK2B*
Focal adhesion	17	*PDGFRA*, *XIAP*, *VAV3*, *LAMC2*, *ITGB4*, *PPP2R5B*, *PPP2R5C*, *RASGRF1*	*PIK3C2B*, *PIK3R5*, *THBS2S*, *ACTN3*, *VCL*, *BLK*, *VAV2*, *BIRC2*, *ILK*
Glycerophospholipid metabolism	16	*AGPAT1*, *MBOAT7*, *CEPT1*, *GLA*, *PNLIPRP2*, *ACHE*, *LYPLA1*, *PLA2G2A*	*AGPAT4*, *CDIPT*, *CHPT1*, *PCYT1B*, *PLA2G2D*, *TAZ*, *PAFAH1B3*, *PLAAT1*
Jak-STAT	14	*PIM1*, *PIAS1*, *IL9R*, *IL21R*, *EPOR*, *PTPN6*	*PIK3C2B*, *PIK3R5*, *BLK*, *SOCS5*, *IFNA8*, *IL4*, *IL17C*, *GFAP*
Oxidative phosphorylation	10	*COX4I1*, *COX6A1*, *COX7B*, *NDUFB3*	*ATP5O*, *ATP5D*, *COX7A1*, *NDUFA13*, *NDUFB4*, *E2IG2*

Caspase-3 is involved in the final stages of apoptosis, participating in the amplification of intracellular apoptotic signals as a consequence of the caspase cascade induced by both intrinsic and extrinsic signaling (26). In the present study, it was found that HG prevents caspase-3 activation and, therefore, apoptosis, which explains the increased chemoresistance to cisplatin (Fig. 1). HG induces apoptosis in normal cells; however, in cancer cells, HG prevents a variety of proapoptotic mechanisms and promotes their proliferation and invasiveness (4,6,28). Additionally, the microarray analysis indicated that HG prevents the cytotoxic action of cisplatin through the increased expression of genes related to cell survival. (*TNFSF7* and *TRAF1*) (Table II) (21), and inhibition of apoptosis (*XIAP* and *BCL2L2*) (Table II) (22,23), together with diminished expression of proapoptotic factors (*BIK*, *PDCD8*, *PDCD5*, *BNIP1*, *DAPK1* and *CCAR2*) (24,25). The overexpression of *BCL2L2* has been associated with an aggressive and radioresistant BC phenotype (22).

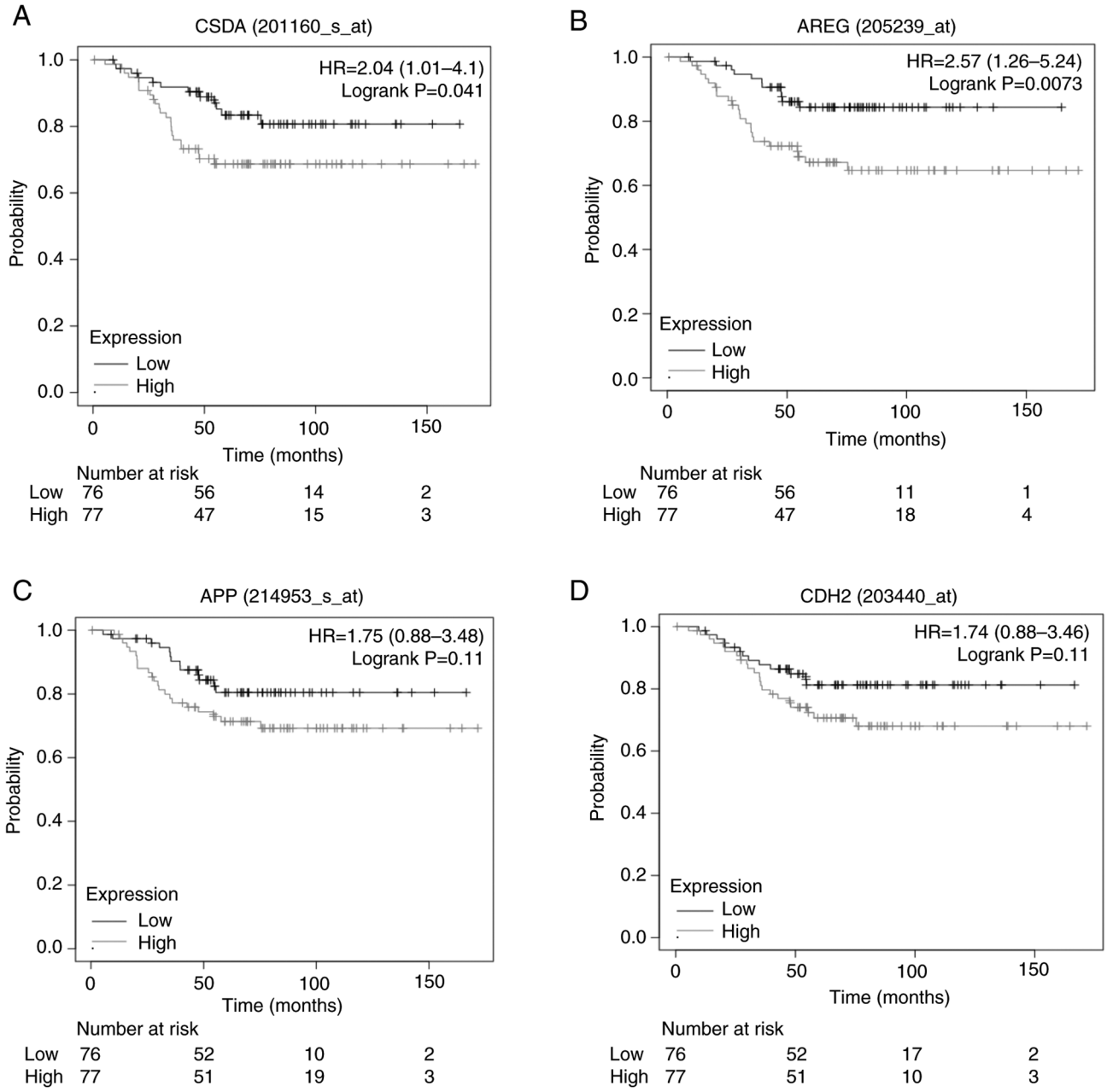


Figure 5. Prognostic biomarkers in hyperglycemia. (A-D) KM survival curves were performed using the KM-plotter platform, considering the mRNA expression levels of (A) *CSDA* (*YBX3*), (B) *AREG*, (C) *APP* and (D) *CDH2* for patients with breast cancer, negative to estrogen, progesterone, and HER2 receptors for IHC and microarrays. KM, Kaplan-Meier; HR, hazard ratio.

Genes involved in metabolism are associated with chemoresistance. Diabetes and hyperglycemia are frequently associated with metabolic disorders. The data suggest that cancer metabolism is intimately linked to drug resistance. The enrichment analysis indicates the differential expression of numerous genes for components of membranes and ribosomes in HG conditions. The first is related to metabolite and ion transporters, and suggests the reprogramming of solute interchange (ions and nutrients) through the cell membranes. The second could be associated with the increased synthesis of proteins.

The reprogramming of membrane transport is suggested because of changes in the expression of 27 solute carrier transporters (SLC) and 10 ATP-dependent transporters in the HG condition (Tables II, SI and SII). The overexpression of SLC that controls the entry of essential amino acids, monocarboxylates, vitamins, glucose, nucleotides and organic cations indicates an increased flux of nutrients, favoring the biosynthetic and energetic demands of cancer cells. The SLC may be novel therapeutic targets and predictive markers of chemoresistance. Among the transporter-coding genes upregulated in the HG condition, *SLC6A6* (4.05 fold) and *SLC39A7* (1.57-fold) have been related to multidrug and cisplatin resistance in colorectal and non-small cell lung cancers (16,29).

The dysregulation of genes coding for ribosomal proteins promotes BC metastasis. Among them, *RPS13* was upregulated more than 2-fold during HG treatment and promoted drug resistance in gastric cancer cells, suppressing apoptosis (17).

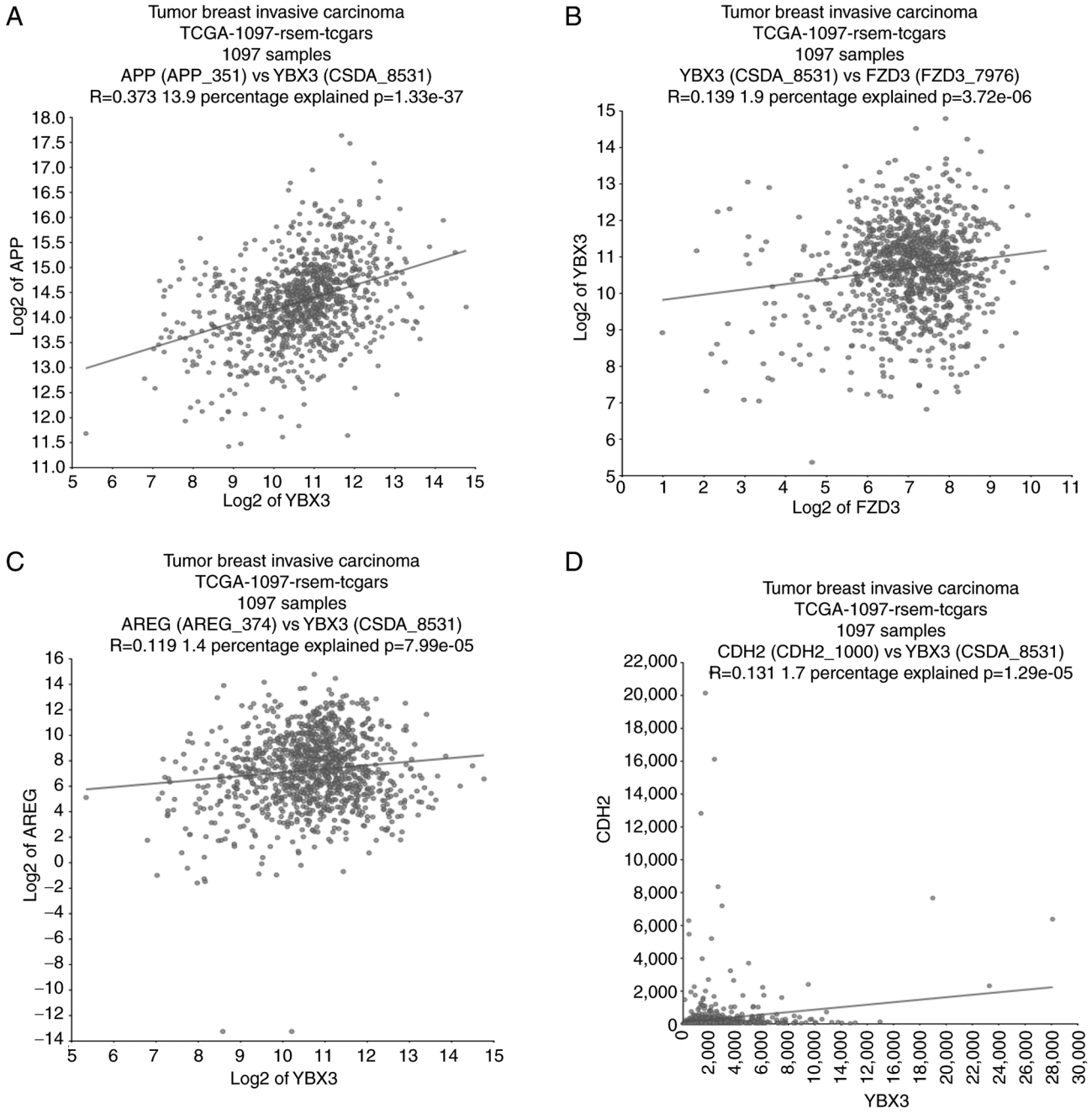


Figure 6. Correlation analysis of gene hubs. (A-D) Correlation analysis of gene expression was performed using the R2 Genomics platform (http://r2.amc.nl) in a cohort of 1,097 patients diagnosed with breast invasive carcinoma (TCGA), aged 26 to 90 years, with heterogeneous hormone receptor status (ER^+ 71.7%, ER^- 22%, PR^+ 63.7%, PR^- 31.4%, $HER2^+$ 14%, and $HER2^-$ 51.3%), and metastatic condition (M0 82.6%, MX 14.8% and M1 2%). Scatter plots show the relationships between (A) *APP* and *YBX3*, (B) *YBX3* and *FZD3*, (C) *AREG* and *YBX3*, and (D) *CDH2* and *YBX3*. Each plot includes a regression line, the Pearson correlation coefficient (R), and the statistical significance (P-value). TCGA, The Cancer Genome Atlas.

Recently, changes in lipid metabolism have been recognized as important mediators of drug resistance. The gene coding for 1-acylglycerol-3-phosphate O-acyltransferase 1 (*AGPAT1*) was the most highly overexpressed in HG. It is highly expressed in breast tumor tissues, and it has been proposed as a component of a gene signature for prognosis in BC (30). More studies are required to determine its role in chemoresistance under HG conditions; some members of the *AGPAT* gene family are upregulated in multiple cancers and are associated with drug resistance and poor prognosis (31).

Crosstalk between different oncogenic signaling pathways in hyperglycemia. The metabolic alterations and changes in gene expression induced by HG suggest the implication of multiple signaling pathways that favor an aggressive phenotype and chemoresistance in MDA-MB-231 cells. RT-qPCR confirmed the overexpression of *TSPAN1* and *FZD3* genes, and several studies suggested their role in cancer progression and chemoresistance. TSPAN-1 promotes the proliferation and development of a migratory-invasive phenotype through the induction of EMT and activation of the PI3K/Akt signaling (32). In addition, the suppression of *TSPAN1* expression prevented BC

tumor growth in mice (18). These data are in agreement with the high expression of TSPAN1 and FZD3 proteins in breast ductal carcinoma in women of reproductive age (Fig. 3).

The finding that *FZD3* and other members of the Wnt canonical signaling [*WNT1, FZD-4,* disheveled 2 (*DVL2*), lymphoid enhancer factor 1 (*LEF1*) and *LRP8*] were overexpressed in a hyperglycemic microenvironment indicates the participation of Wnt signaling in the promotion of an aggressive and chemoresistant phenotype by hyperglycemia, which was supported by the enrichment and the PPI analyses. The altered expression of genes of the Wnt pathway has been related to cancer progression and poor prognosis (33,34). WNT1 can induce transformation of the mouse mammalian cell line C57MG (34). The expression of *WNT1* and *LEF1* is upregulated in human breast carcinoma (35). Whereas the upregulation of *FZD4* in glioma cells is correlated with resistance to drug-induced cell death, partly due to the activation of Wnt/β-catenin and downregulation of proapoptotic genes (*CASP3* and *PDCD4*) (36). The silencing of *LRP8* by interference RNA attenuates Wnt/β-catenin, decreases the metastatic potential, and sensitizes BC cells to chemotherapy (37). As a consequence of the activation of the Wnt pathway, LEF-1 and T cell factor (TCF) form a complex and activate the expression of genes such as *MDR1*, *C-MYC*, *MET*, *MMP7*, *C-JUN* and *CCND1*, contributing to carcinogenesis and tumor progression in several cancers (33,35). In MCF7 BC cells, LEF1 induces resistance to docetaxel (DTX), and the inhibition of LEF1 with quercetin reestablishes sensitivity to DTX (38). LEF1 is a transcription factor that controls gene expression dependent or independent of Wnt/β-catenin signaling and increases the expression of EMT effectors, such as snail, vimentin and N-cadherin; the gene that encodes N-cadherin, *CDH2*, was also found to be overexpressed in the HG condition (Table SI). The potential role of the Wnt pathway in the promotion of BC under hyperglycemic conditions requires further studies.

The non-canonical signaling of Wnt can also be implicated in the promotion of BC by hyperglycemia. Two genes that encode CDC42 effectors were overexpressed by 2-fold in HG conditions, including CDC42 binding protein kinase alpha and CDC42 small effector 1. The binding of WNT1 with FZD-3 induces the activation of CDC42 in a β-catenin independent signaling, and CDC42 induces the reorganization of the cytoskeleton and cell migration (39).

As the PPI indicates, the ATM-dependent DNA-repairing pathway is of special interest, considering that platinum salts are DNA-damaging agents. *ATM* improves the ability to repair double-strand DNA breaks and can lead to increased resistance to DNA-damaging chemotherapeutic agents, such as platinum salts (40).

Potential genes associated with chemoresistance induced by hyperglycemia. Through the evaluation of hub genes with a greater number of interactions (Fig. 4), the survival of TNBC patients using the KM plotter (Fig. 5) and coexpression analysis (Fig. 6), the authors propose *YBX3* as a central regulator positively correlated with *AREG*, *APP* and *FZD3*, suggesting that these genes may participate in a signaling network that promotes proliferation, invasion and therapy resistance under hyperglycemic conditions. In particular, *YBX3* and *AREG* showed significant prognostic value, as their high expression was associated with reduced survival in patients with BC, highlighting their potential as biomarkers of poor outcome (Fig. 5).

By contrast, *APP* and *CDH2* did not reach statistical significance in survival analyses, but coexpression studies demonstrated that both genes are positively correlated with *YBX3* (Fig. 6). This finding suggests that *APP* and *CDH2* may not act as independent prognostic markers, but rather as cooperative elements within *YBX3*-driven regulatory networks, thereby contributing indirectly to tumor progression and aggressiveness. Importantly, recent studies have shown that *YBX3* is overexpressed in multiple cancer types and contributes to chemoresistance by regulating transcriptional and translational programs involved in EMT, proliferation, and survival pathways (19,41,42). Moreover, YBX3 regulates the expression of growth factors and ligands such as *AREG*, creating a positive feedback loop that amplifies growth factor signaling, enhances EMT, and promotes chemoresistance (43).

AREG is the primary EGFR ligand in MDA-MB-231 cells, and its binding to EGFR promotes BC growth and metastasis (44). APP overexpression drives EMT, proliferation and migration/invasion in BC cells, and it has been proposed as a risk factor for lymph node metastasis and poor prognosis in non-luminal BCs, including TNBC (45). CDH2 is a mesenchymal marker induced by EMT that facilitates migration and invasion, and its high expression correlates with poor prognosis in invasive micropapillary BC (46,47).

Taken together, these findings suggest that while *AREG* and *CDH2* emerge as potential prognostic biomarkers, *APP* and *CDH2* may act primarily as modulators of *YBX3*-driven transcriptional networks that support tumor progression rather than serving as independent prognostic indicators. Nevertheless, despite these associations, the current evidence remains insufficient to establish these hub genes as reliable biomarkers, underscoring the need for further validation in larger patient cohorts and in-depth functional studies.

It must be considered that an increase in the mRNA level of a gene is not always followed by an increase in the codified protein, and the protein generally realizes a function in metabolism, secretion, or gene expression regulation. This situation limits the conclusions of the estimations of the OS based on mRNA values, as our data were derived from the KM plot analysis.

Therapeutic implications and resistance bypass strategies. The present results provide a foundation for therapeutic strategies aimed at overcoming hyperglycemia-induced chemoresistance in TNBC. Previous studies have shown that inhibitors or interfering RNAs targeting *YBX3* increase chemosensitivity, highlighting a promising approach for TNBC (19,42). Other potential therapeutic targets include metabolic reprogramming and transporter activity, considering the *SLC6A6*, *SLC39A7* and *RPS13* genes (16,17,29), which are overexpressed in HG and aforementioned. Pharmacological inhibition of these transporters, or modulation of glucose and lipid metabolism, could sensitize TNBC cells to chemotherapy. Combined strategies that target metabolic and oncogenic signaling pathways may prove particularly effective. The inhibition of the Wnt/β-catenin pathway or ATM-mediated DNA repair, in

combination with chemotherapy, could synergistically reduce tumors. These findings support a framework for personalized combinatorial therapies in diabetic patients with BC, integrating metabolic modulators, inhibitors of *YBX3*-regulated networks, and conventional chemotherapeutics to overcome resistance and improve clinical outcomes.

Limitations of the present study. The present study has potential limitations. It was based on the analysis of the changes induced by HG in an invasive BC cell line, using an *in vitro* experimental and bioinformatics approach. Although the MDA-MB-231 cell line has been widely used as a model of invasive BC, it does not represent the genetic heterogeneity of invasive breast tumors. Therefore, the current findings need to be validated in other experimental models and clinical cohorts. However, the present study provides important insights and allows us to better understand the behavior of this type of cancer under HG conditions, as well as to identify potential signaling pathways and genes associated with chemoresistance and prognosis in patients with T2DM.

Although the use of *HPRT* as a housekeeping gene is considered unreliable for comparing the gene expression between cancerous and non-cancerous tissues (48), this gene has been recommended in hyperglycemic conditions (13), and its expression is moderately stable in BC cell lines (12), although in hyperglycemic conditions, it has been validated in other types of cells. Therefore, the use of an additional reference gene is recommended to further consolidate the overexpression of *TSPAN* and *FZD3* genes.

The present findings and bibliographic references suggest that *TSPAN1* and *FZD3* play an important role in the induction of chemoresistant and invasive phenotypes by HG (18,32). However, gene knockdown experiments are required to better understand their roles.

The clinical implications were partially validated using public patient datasets and informatics platforms; however, these platforms are generally based on non-diabetic patients, and the estimation of the effect of selected overexpressed genes on OS was therefore performed in non-diabetic conditions. These results should be interpreted with caution, highlighting the need for further validation in diabetic patient cohorts.

Additionally, both diabetes and cancer are complex processes involving multiple genetic and environmental contexts; therefore, further studies are required to validate the clinical implications of our findings. These include validation at both protein (western blotting and IHC) and mRNA (RT-qPCR) levels of overexpressed genes (*FZD3* and *TSPAN1*), as well as of potential genes associated with chemoresistance and prognosis (*AREG* and *YBX3*) in breast tumor tissues of diabetic patients.

In addition, changes in gene expression and the induction of cisplatin chemoresistance by diabetes in a mouse model of syngeneic BC are currently studied, and patient-derived organoids can be used to analyze cisplatin action under HG conditions in human tissues. Finally, the correlation of the selected genes and clinical outcomes should be studied in other patient cohorts, preferably in diabetic patients with BC.

In conclusion, these data indicate that alterations in gene expression induced by hyperglycemia lead to changes in the metabolism of cancer cells, affecting a variety of processes that promote a more aggressive phenotype through the activation of Wnt/β-catenin, NF-κB survival, angiogenesis and PI3K/AKT signaling, contributing to enhanced proliferation, migration, invasion and inhibition of apoptosis. Some potential biomarkers of cisplatin resistance under hyperglycemia could be *AREG* and *YBX3*.

Acknowledgements

The authors would like to thank Ms Lorena Chávez, Dr José Luis Santillán, Mr Simón Guzmán and Dr Jorge Ramírez for performing the microarray analysis at the Instituto de Fisiología Celular, National Autonomous University of Mexico. The authors thank student Mr Jael Gutiérrez Savedra for his technical assistance, and Dr Leticia Moreno Fierros for her technical advice [both are affiliated to the National Autonomous University of Mexico (UNAM), FES-Iztacala].

Funding

The present study was supported by the Programa de Apoyo a Proyectos de Investigación e Innovación Tecnológica *(PAPIIT),* Dirección General de Apoyo al Personal Académico (DGAPA), Universidad Nacional Autónoma de México (UNAM), (grant nos. IN223121 and IN220024), by the Financing for Research of Women Scientists (grant no. FICDTEM-2023-56) and by the Fiscal Resources Program for Research of the National Institute of Pediatrics (grant no. 2020/016).

Availability of data and materials

The data generated in the present study may be found in the Gene Expression Omnibus under accession number GSE136277 or at the following URL: https://www.ncbi.nlm.nih.gov/geo/query/acc.cgi?acc=GSE136277. The data generated in the present study are included in the figures and/or tables of this article.

Authors' contributions

ARVR, MGMH and LABG contributed to the conception and design of the study. ARVR, MGMH, LAFL, MÁVF, RREG and JRPB performed material preparation, data collection and analysis. ARVR and LABG wrote the first draft of the manuscript. All authors commented on previous versions of the manuscript. All authors read and approved the final version of the manuscript. ARVR and LABG confirm the authenticity of all the raw data.

Ethics approval and consent to participate

Not applicable.

Patient consent for publication

Not applicable.

Competing interests

The authors declare that they have no competing interests.

References

1. Ryu TY, Park J and Scherer PE: Hyperglycemia as a risk factor for cancer progression. Diabetes Metab J 38: 330-336, 2014.
2. Varghese E, Samuel SM, Líšková A, Samec M, Kubatka P and Büsselberg D: Targeting glucose metabolism to overcome resistance to anticancer chemotherapy in breast cancer. Cancers (Basel) 12: 2252, 2020.
3. Qiu J, Zheng Q and Meng X: Hyperglycemia and chemoresistance in breast cancer: From cellular mechanisms to treatment response. Front Oncol 11: 628359, 2021.
4. Flores-López LA, Martínez-Hernández MG, Viedma-Rodríguez R, Díaz-Flores M and Baiza-Gutman LA: High glucose and insulin enhance uPA expression, ROS formation and invasiveness in breast cancer-derived cells. Cell Oncol (Dordr) 39: 365-378, 2016.
5. Bergandi L, Mungo E, Morone R, Bosco O, Rolando B and Doublier S: Hyperglycemia promotes chemoresistance through the reduction of the mitochondrial DNA damage, the Bax/Bcl-2 and Bax/Bcl-XL ratio, and the cells in sub-G1 phase due to antitumoral drugs induced-cytotoxicity in human colon adenocarcinoma cells. Front Pharmacol 9: 866, 2018.
6. Viedma-Rodríguez R, Martínez-Hernández MG, Flores-López LA and Baiza-Gutman LA: Epsilon-aminocaproic acid prevents high glucose and insulin induced-invasiveness in MDA-MB-231 breast cancer cells, modulating the plasminogen activator system. Mol Cell Biochem 437: 65-80, 2018.
7. Huang Y, Hong W and Wei X: The molecular mechanisms and therapeutic strategies of EMT in tumor progression and metastasis. J Hematol Oncol 15: 129, 2022.
8. Panigrahi G, Candia J, Dorsey TH, Tang W, Ohara Y, Byun JS, Minas TZ, Zhang AL, Ajao A, Cellini A, *et al*: Diabetes-associated breast cancer is molecularly distinct and shows a DNA damage repair deficiency. JCI Insight 8: e170105, 2023.
9. Ashrafizadeh M, Zarrabi A, Hushmandi K, Kalantari M, Mohammadinejad R, Javaheri T and Sethi G: Association of the epithelial-mesenchymal transition (EMT) with cisplatin resistance. Int J Mol Sci 21: 4002, 2020.
10. Frossard M, Blank D, Joukhadar Ch, Bayegan K, Schmid R, Luger A and Müller M: Interstitial glucose in skeletal muscle of diabetic patients during an oral glucose tolerance test. Diabet Med 22: 56-60, 2005.
11. Schmittgen TD and Livak KJ: Analyzing real-time PCR data by the comparative C(T) method. Nat Protoc 3: 1101-1108, 2008.
12. Gorji-Bahri G, Moradtabrizi N, Vakhshiteh F and Hashemi A: Validation of common reference genes stability in exosomal mRNA-isolated from liver and breast cancer cell lines. Cell Biol Int 45: 1098-1110, 2021.
13. Liu X, Xie J, Liu Z, Gong Q, Tian R and Su G: Identification and validation of reference genes for quantitative RT-PCR analysis of retinal pigment epithelium cells under hypoxia and/or hyperglycemia. Gene 580: 41-46, 2016.
14. Doncheva NT, Morris JH, Gorodkin J and Jensen LJ: Cytoscape StringApp: Network analysis and visualization of proteomics data. J Proteome Res 18: 623-632, 2019.
15. Chin CH, Chen SH, Wu HH, Ho CW, Ko MT and Lin CY: cytoHubba: identifying hub objects and sub-networks from complex interactome. BMC Syst Biol 8 (Suppl 4): S11, 2014.
16. Yasunaga M and Matsumura Y: Role of SLC6A6 in promoting the survival and multidrug resistance of colorectal cancer. Sci Rep 4: 4852, 2014.
17. Shi Y, Zhai H, Wang X, Han Z, Liu C, Lan M, Du J, Guo C, Zhang Y, Wu K and Fan D: Ribosomal proteins S13 and L23 promote multidrug resistance in gastric cancer cells by suppressing drug-induced apoptosis. Exp Cell Res 296: 337-346, 2004.
18. Garcia-Mayea Y, Mir C, Carballo L, Sánchez-García A, Bataller M and ME LL: TSPAN1, a novel tetraspanin member highly involved in carcinogenesis and chemoresistance. Biochim Biophys Acta Rev Cancer 1877: 188674, 2022.
19. Tong C, Qu K, Wang G, Liu R, Duan B, Wang X and Liu C: Knockdown of DNA-binding protein A enhances the chemotherapy sensitivity of colorectal cancer via suppressing the Wnt/β-catenin/Chk1 pathway. Cell Biol Int 44: 2075-2085, 2020.
20. Lánczky A and Győrffy B: Web-based survival analysis tool tailored for medical research (KMplot): Development and implementation. J Med Internet Res 23: e27633, 2021.
21. Liu N, Sheng X, Liu Y, Zhang X and Yu J: Increased CD70 expression is associated with clinical resistance to cisplatin-based chemotherapy and poor survival in advanced ovarian carcinomas. Onco Targets Ther 6: 615-619, 2013.
22. Hartman ML and Czyz M: BCL-w: Apoptotic and non-apoptotic role in health and disease. Cell Death Dis 11: 260, 2020.
23. Bano D and Prehn JHM: Apoptosis-inducing factor (AIF) in physiology and disease: The tale of a repented natural born killer. EBioMedicine 30: 29-37, 2018.
24. Zheng HC: The molecular mechanisms of chemoresistance in cancers. Oncotarget 8: 59950-59964, 2017.
25. Gozuacik D, Bialik S, Raveh T, Mitou G, Shohat G, Sabanay H, Mizushima N, Yoshimori T and Kimchi A: DAP-kinase is a mediator of endoplasmic reticulum stress-induced caspase activation and autophagic cell death. Cell Death Differ 15: 1875-1886, 2008.
26. Porter AG and Jänicke RU. Emerging roles of caspase-3 in apoptosis. Cell Death Differ 6: 99-104. 1999.
27. Viedma-Rodríguez R, Martínez-Hernández MG, Martínez-Torres DI and Baiza-Gutman LA: Epithelial mesenchymal transition and progression of breast cancer promoted by diabetes mellitus in mice are associated with increased expression of glycolytic and proteolytic enzymes. Horm Cancer 11: 170-181, 2020.
28. Vaughn AE and Deshmukh M: Glucose metabolism inhibits apoptosis in neurons and cancer cells by redox inactivation of cytochrome c. Nat Cell Biol 10: 1477-1483, 2008.
29. Wu DM, Liu T, Deng SH, Han R and Xu Y: SLC39A4 expression is associated with enhanced cell migration, cisplatin resistance, and poor survival in non-small cell lung cancer. Sci Rep 7: 7211, 2017.
30. Ren X, Cui H, Wu J, Zhou R, Wang N, Liu D, Xie X, Zhang H, Liu D, Ma X, *et al*: Identification of a combined apoptosis and hypoxia gene signature for predicting prognosis and immune infiltration in breast cancer. Cancer Med 11: 3886-3901, 2022.
31. Wen P, Wang R, Xing Y, Ouyang W, Yuan Y, Zhang S, Liu Y and Peng Z: The prognostic value of the GPAT/AGPAT gene family in hepatocellular carcinoma and its role in the tumor immune microenvironment. Front Immunol 14: 1026669, 2023.
32. Wu Y, Chen W, Gong Y, Liu H and Zhang B: Tetraspanin 1 (TSPAN1) promotes growth and transferation of breast cancer cells via mediating PI3K/Akt pathway. Bioengineered 12: 10761-10770, 2021.
33. Merikhian P, Eisavand MR and Farahmand L: Triple-negative breast cancer: Understanding Wnt signaling in drug resistance. Cancer Cell Int 21: 419, 2021.
34. Wong GT, Gavin BJ and McMahon AP: Differential transformation of mammary epithelial cells by Wnt genes. Mol Cell Biol 14: 6278-6286, 1994.
35. Ayyanan A, Civenni G, Ciarloni L, Morel C, Mueller N, Lefort K, Mandinova A, Raffoul W, Fiche M, Dotto GP and Brisken C: Increased Wnt signaling triggers oncogenic conversion of human breast epithelial cells by a Notch-dependent mechanism. Proc Natl Acad Sci USA 103: 3799-3804, 2006.
36. Jin X, Jeon HY, Joo KM, Kim JK, Jin J, Kim SH, Kang BG, Beck S, Lee SJ, Kim JK, *et al*: Frizzled 4 regulates stemness and invasiveness of migrating glioma cells established by serial intracranial transplantation. Cancer Res 71: 3066-3075, 2011.
37. Lin CC, Lo MC, Moody R, Jiang H, Harouaka R, Stevers N, Tinsley S, Gasparyan M, Wicha M and Sun D: Targeting LRP8 inhibits breast cancer stem cells in triple-negative breast cancer. Cancer Lett 438: 165-173, 2018.
38. Prieto-Vila M, Shimomura I, Kogure A, Usuba W, Takahashi RU, Ochiya T and Yamamoto Y: Quercetin inhibits Lef1 and resensitizes docetaxel-resistant breast cancer cells. Molecules 25: 2576, 2020.
39. Tümen D, Heumann P, Huber J, Hahn N, Macek C, Ernst M, Kandulski A, Kunst C and Gülow K: Unraveling cancer's Wnt signaling: Dynamic control through protein kinase regulation. Cancers (Basel) 16: 2686, 2024.
40. Galland L, Ballot E, Mananet H, Boidot R, Lecuelle J, Albuisson J, Arnould L, Desmoulins I, Mayeur D, Kaderbhai C, *et al*: Efficacy of platinum-based chemotherapy in metastatic breast cancer and HRD biomarkers: Utility of exome sequencing. NPJ Breast Cancer 8: 28. 2022.
41. Wang C, You Z, He Y and Chen X: Identification of RNA-binding protein YBX3 as an oncogene in clear cell renal cell carcinoma. Funct Integr Genomics 23: 225, 2023.
42. Sun Y, Li Z, Wang W, Zhang X, Li W, Du G, Yin J, Xiao W and Yang H: Identification and verification of YBX3 and its regulatory gene HEIH as an oncogenic system: A multidimensional analysis in colon cancer. Front Immunol 13: 957865, 2022.

43. Panupinthu N, Yu S, Zhang D, Zhang F, Gagea M, Lu Y, Grandis JR, Dunn SE, Lee HY and Mills GB: Self-reinforcing loop of amphiregulin and Y-box binding protein-1 contributes to poor outcomes in ovarian cancer. Oncogene 33: 2846-2856, 2014.
44. Bolitho C, Moscova M, Baxter RC and Marsh DJ: Amphiregulin increases migration and proliferation of epithelial ovarian cancer cells by inducing its own expression via PI3-kinase signaling. Mol Cell Endocrinol 533: 111338, 2021.
45. Wu X, Chen S and Lu C: Amyloid precursor protein promotes the migration and invasion of breast cancer cells by regulating the MAPK signaling pathway. Int J Mol Med 45: 162-174, 2020.
46. Cao ZQ, Wang Z and Leng P: Aberrant N-cadherin expression in cancer. Biomed Pharmacother 118: 109320, 2019.
47. Ge R, Wang Z, Wu S, Zhuo Y, Otsetov AG, Cai C, Zhong W, Wu CL and Olumi AF: Metformin represses cancer cells via alternate pathways in N-cadherin expressing vs N-cadherin deficient cells. Oncotarget 6: 28973-28987, 2015.
48. Townsend MH, Felsted AM, Ence ZE, Piccolo SR, Robison RA and O'Neill KL: Falling from grace: HPRT is not suitable as an endogenous control for cancer-related studies. Mol Cell Oncol 6: 1575691, 2019.

Copyright © 2025 Viedma-Rodríguez et al. This work is licensed under a Creative Commons Attribution-NonCommercial-NoDerivatives 4.0 International (CC BY-NC-ND 4.0) License.